POLITECNICO DI TORINO
Repository ISTITUZIONALE

Optimal Battery Scheduling for Self-Sufficiency in Energy Communities: A Case Study on the PVZEN Microgrid

Original
Optimal Battery Scheduling for Self-Sufficiency in Energy Communities: A Case Study on the PVZEN Microgrid / Ciocia, A., Malgaroli, G., Travaglini, M.L., D'Angola, A., Spertino, F.. - (2025), pp. 1-6. (2025 IEEE International Conference on Environment and Electrical Engineering and 2025 IEEE Industrial and Commercial Power Systems Europe, EEEIC / I and CPS Europe 2025 grc 2025) [10.1109/EEEIC/ICPSEurope64998.2025.11169217].

Availability:
This version is available at: 11583/3005293 since: 2025-11-19T17:08:05Z

Publisher:
Institute of Electrical and Electronics Engineers Inc.

Published
DOI:10.1109/EEEIC/ICPSEurope64998.2025.11169217

Terms of use:

This article is made available under terms and conditions as specified in the corresponding bibliographic description in the repository

Publisher copyright
IEEE postprint/Author's Accepted Manuscript

©2025 IEEE. Personal use of this material is permitted. Permission from IEEE must be obtained for all other uses, in any current or future media, including reprinting/republishing this material for advertising or promotional purposes, creating new collecting works, for resale or lists, or reuse of any copyrighted component of this work in other works.

(Article begins on next page)

27 November 2026

Optimal Battery Scheduling for Self-Sufficiency in Energy Communities: A Case Study on the PVZEN Microgrid

Alessandro Ciocia, Gabriele Malgaroli, Maria Lara Travaglini, Filippo Spertino

Dipartimento Energia "Galileo Ferraris", Politecnico di Torino, Torino, Italy

{alessandro.ciocia, gabriele.malgaroli, maria.travaglini, filippo.spertino}@polito.it

Antonio D'Angola

Scuola di Ingegneria, Università della Basilicata, Potenza, Italy

antonio.dangola@unibas.it

Abstract

This paper presents a centralized energy management strategy aimed at maximizing the self-sufficiency of a real microgrid, developed and tested within the PhotoVoltaic Zero Energy Network (PVZEN) laboratory at Politecnico di Torino. A non-linear optimization algorithm is implemented to determine the optimal charging and discharging profiles of the battery systems. The strategy allows energy sharing among users and ensures coordinated operation of the storage units as a virtual aggregated battery. The strategy is tested through simulations based on hourly data and results compared with a baseline case reflecting conventional inverter behaviour. Simlulation results demonstrate a significant increase in energy self-sufficiency — from 58% to 72% — and self-consumption — from 70% to 87% — together with improved battery availability and reduced grid dependence.

Keywords: Photovoltaic System, Energy Community, Battery Energy Storage Systems, Optimization, Self-Sufficiency

1 Introduction

Microgrids represent an innovative solution to integrate renewable energy sources with high reliability and sustainability, contributing to reduced transmission losses and improved energy efficiency [1]. Typically, a microgrid consists of a localized power subsystem with a limited number of distributed energy resources, functioning either in grid-connected or islanded mode [2].

Effective energy management within microgrids is essential to address the variability of Renewable Energy Sources (RES) and to optimize resource utilization. Management

strategies are broadly categorized as centralized [3], decentralized [4] [5], and hierarchical [6] [7], depending on the degree of control centralization and user interaction.

Centralized approaches have long been predominant. They rely on a central controller to manage loads, RES, and storage systems with the primary goal of maximizing community self-sufficiency. Many such studies focus on strategies to allocate surplus energy among users with storage capabilities. For example, the work of [3] presents a centralized model that coordinates photovoltaic generation and Energy Storage Systems (ESSs) of users to form a Virtual Community Energy Storage (VCES). The model operates on two levels: day-ahead scheduling, based on forecasted load, generation, and SOC, and real-time adjustments, considering actual data. The results of the study demonstrate that the system successfully stores 29.5% of surplus energy and supplies 37.3% of deficits.

Another approach is described in [8], where surplus is allocated considering ESSs efficiency at varying load levels and optimal operating points. This method improves performance by balancing surplus and deficits across time and users, resulting in lower net surplus and improved efficiency. This work shows that centralized control yields a 21% efficiency improvement and identifies substantial benefits in communities with as few as 5 to 20 members.

The present study seeks to maximize the utilization of PV generation and storage through a coordinated, centralized management framework. A non-linear optimization function is employed to determine the optimal charging and discharging profiles of individual ESSs, aiming to maximize overall self-sufficiency. The residual battery capacity is not prioritized as criterion for energy allocation, being instead considered as physical constraint of optimization, but the direction of power flows is instead solely governed by the objective of maximizing system-wide self-sufficiency, which is itself dependent on the battery power flows.

Similar to the study [8], the model allows direct energy sharing among units, enabling coordinated actions such as discharging one unit's battery to support another unit's load, even if it has local generation and unused capacity. This results in synchronized SOC profiles across all storage units, effectively treating them as a single virtual battery. Performance is evaluated against a baseline scenario in which each unit acts independently, confirming that the strategy aligns with centralized energy community management principles.

2 The PVZEN laboratory

The PVZEN is an experimental laboratory for energy communities set up on the campus of the Politecnico di Torino [9]. The laboratory emulates a microgrid with PV generators, electro-chemical storage systems and electrical loads, including heat pumps for air conditioning (heating/cooling) of laboratory rooms and generic appliances such as lamps and electronic devices. The PVZEN laboratory allows the testing of both off-grid operation and energy community operation for users.

In the PVZEN, users are connected in parallel to each other and to the grid. This

configuration allows the users to share their surplus with each other in case of an energy surplus, and to draw energy from the external grid in case of deficit.

The PV system is subdivided into three photovoltaic generators, with a total peak power of 11.1 kWp. The peak power expressed in Wp refers to an irradiance value of $G_{\mathrm{STC}} = 1000\ \mathrm{W/m^2}$. The mono-crystalline silicon (m-Si) PV modules have a rated efficiency of 21.4% and a peak power of 370 Wp. The optimal orientation of PV modules in the northern hemisphere is towards the south, with the tilt angle being a function of latitude. This configuration maximises energy production. In the PVZEN system the PV arrays have been intentionally installed under non-optimal conditions, in order to represent diverse installation scenarios on the rooftops of apartment buildings. The first PV generator is equipped with 12 modules (peak power of 4.44 kWp) with an orientation of $-64°$ (south-east) relative to south (where $-90°$ is east, $0°$ is south, and $90°$ is west). The second PV generator comprises six modules (peak power of 2.22 kWp) with an orientation of $116°$ (north-west). The third PV generator comprises 12 modules (peak power of 4.44 kWp), which are subdivided into two 6-module sub-generators: the first sub-generator has an orientation of $-64°$ (SE) relative to south, while the second sub-generator has an orientation of $116°$ (NW) relative to South. All PV modules have a tilt angle of approximately $10°$. Consequently, due to suboptimal installation conditions, irradiance is consistently below $1000\ \mathrm{W/m^2}$, thereby precluding the attainment of peak power by the arrays.

A fourth unit, consisting of a centralized 60 kWh storage system, has been recently added to the community. However, as it is currently in the starting phase, it is not included in the simulations presented in this work.

Each user is equipped with four lithium batteries, with a nominal energy capacity of 2.4 kWh per unit. The total nominal energy capacity allocated to each user is 9.6 kWh, thus yielding an aggregate microgrid capacity of 28.8 kWh. The batteries have a nominal voltage of 48 V, a charge capacity of 50 Ah, and a maximum charging/discharging current of 100 A for one minute. The Depth of Discharge (DOD) is 90%, which implies a minimum SOC of 10%.

To perform the DC/AC conversion with sinusoidal output voltage ($230\ \mathrm{V_{rms}}$, 50 Hz) each user is equipped with a 5 kW converter, designed to operate in both grid-connected and off-grid modes. Each device is equipped with an AC input, allowing connection to the grid, and an AC output for the connection to the loads. The direct current (DC) power from the PV array can supply the storage system - thus enabling battery charging - through a Maximum Power Point Tracker (MPPT) that performs the DC/DC conversion. The DC/AC stage can also operate by receiving AC power from the utility grid in order to charge the lithium batteries on the DC side. Finally, the power injection into the grid is set to zero.

To enable off-grid mode operation, the connection to the grid can be disabled.

Regarding the electrical loads, the three generation units supply a resistor bench that can reproduce known profiles of residential or office users, including heat pumps. Each resistor can dissipate a maximum power of 4 kW [10]. A scheme of the PVZEN microgrid

is provided in Fig. 1.

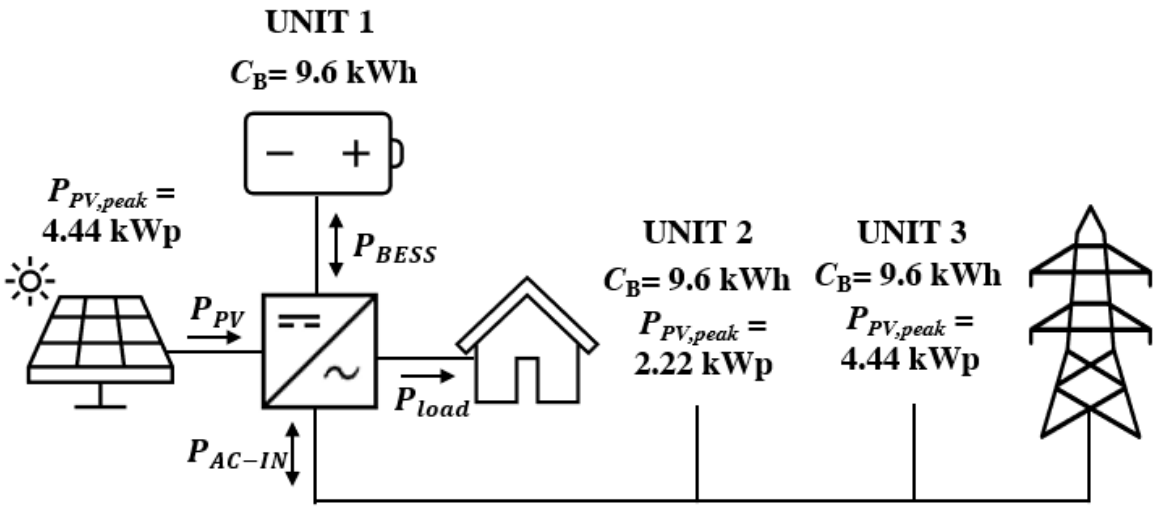

Figure 1: Scheme of PVZEN laboratory

3 PVZEN monitoring system

The monitoring architecture is structured in three main programs that operate continuously and in parallel, both with one another and with an SQL database, which allows simultaneous data access by multiple users without interference. The programs are loaded on a central server, which communicates with the power converters via Modbus TCP/IP protocol.

The first Matlab program reads data minute-by-minute from the power converters through the Modbus serial communication, re-organizes and then loads them into the SQL database.

The second Matlab program reads the data stored in the database and determines the power flows within microgrid; if required, it also performs an optimization and sends the resulting control variable back to the database for following uses.

The third Matlab program reads the processed data from the database and transmits the set-points to the power converters, performing the inverse action of the first program.

The synergistic work of the programs provides for data acquisition, processing and command dispatching to the microgrid, thereby fulfilling the main functionalities of a monitoring system.

Monitoring data are visualized by using Grafana, which is an open source visualization platform. The inclusion of Grafana enables real-time monitoring of microgrid performance. If data are missing, an alert is set on Grafana to notify through a Telegram message.

This system is an example of integration of different communication protocols and programming language database (Modbus, MATLAB, Grafana, MySQL, Telegram) for effective energy monitoring in a microgrid context. The scheme of the monitoring archi-

tecture is provided in Fig. 2.

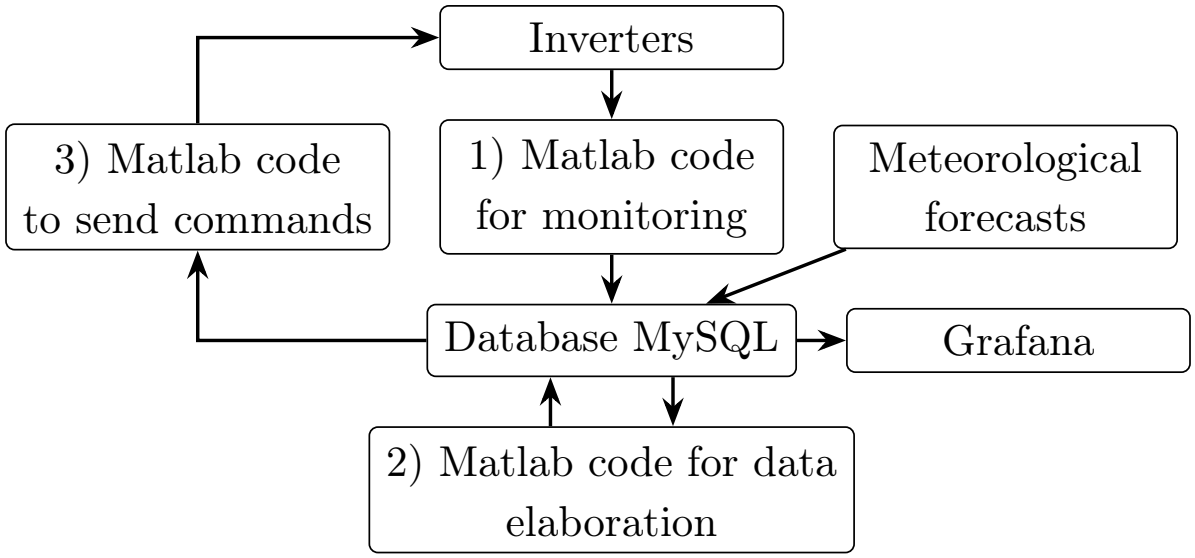

Figure 2: Monitoring architecture of PVZEN

4 Energy models for simulations

The DC power generated by PV modules can be calculated, knowing the irradiance G on the module plane and the air temperature T_{air} [11], according to the Eq. (1):

$$P_{\text{PV}} = P_{\text{nom}} \cdot \frac{G - G_0}{G_{\text{STC}}} \cdot [1 + \gamma_{\text{th}} \cdot (T_{\text{mod}} - T_{\text{mod,STC}})] \cdot \eta \tag{1}$$

P_{nom} is the rated power of the PV system at Standard Test Conditions (STC), i.e., irradiance $G_{\text{STC}} = 1$ kW/m^2 and module temperature $T_{\text{mod,STC}} = 25$ °C; G_0 is the irradiance threshold value below which there is not any PV generation ($\sim 25\ W/m^2$), while γ_{th} is the temperature coefficient expressing the dependence of PV generation on module temperature T_{mod} and η is the PV efficiency, which takes into account several loss factors, such as glass reflection and refraction losses, module soiling, mismatch losses and losses in cables due to Joule effect ($\sim 90\%$). The module temperature is evaluated from T_{air} and G using the Nominal Operating Cell Temperature (NOCT) formula [12].

In DC/AC power converters, losses P_{losses} can be modelled as a function of the output power P_{out}, as reported in Eq. (2).

$$P_{\text{losses}} = k_{\text{quad}} \cdot P_{\text{out}}^2 + k_{\text{lin}} \cdot P_{\text{out}} + P_0 \tag{2}$$

where the factors k_{quad} models the losses proportional to the square of P_{out}, k_{lin} models the losses linearly proportional to P_{out}, and P_0 is the converter self-consumption power [10].

The functioning of a BESS can be described by the evolution of its SOC, defined as the ratio of residual to nominal energy capacity [13]. The SOC at the time instant t can

be evaluated from the SOC at the previous time instant $(t-1)$ using the Eq. (3) and Eq. (4), respectively for the charging and discharging phase:

$$SOC(t) = SOC(t-1) + \frac{|P_{\mathrm{B}}| \cdot \Delta t}{C_{\mathrm{B}}} \cdot \eta_{\mathrm{ch}} - \frac{P_{\text{self-disch}} \cdot \Delta t}{C_{\mathrm{B}}} \tag{3}$$

$$SOC(t) = SOC(t-1) - \frac{|P_B| \cdot \Delta t}{C_B \cdot \eta_{disch}} - \frac{P_{\text{self-discharge}} \cdot \Delta t}{C_B} \tag{4}$$

where P_{B} is the battery power in the time interval Δt, C_{B} is the battery nominal capacity, η_{ch} and η_{disch} are, respectively, the charging and discharging efficiency and $P_{\mathrm{self-disch}}$ is the self-discharged power [14].

5 Power management strategies

The proposed optimised strategy for power management is tested on the PVZEN microgrid through hourly time-step simulations as a study case. The objective of this study is the determination of the power flows in/from the storage systems that maximize the self-sufficiency of the microgrid. Then, the power exchanged by each unit with the grid is calculated through a power balance. The strategy is centralized and it is based on the assumption that each unit can exchange energy with the others. Results are compared to a baseline case, involving the autonomous operation of the units.

5.1 Reference case without centralized control

To evaluate the effectiveness of the proposed optimal energy management strategy, a baseline scenario is considered as reference case, in which each prosumer operates independently. This configuration reflects the default operation of conventional inverter systems. In this scenario, PV generation is primarily used to cover the local load. In case of an energy deficit, the system prioritizes the use of the local battery storage; if the battery is unable to meet the demand, the remaining power requirement is fulfilled by drawing energy from the grid. Conversely, in the presence of a generation surplus, the excess energy is first directed to charge the local battery. Any remaining surplus, after the battery is fully charged, is exported to the grid [15]. According to this sequence, the power exchanged with the grid is computed for each unit by applying the power balance equation, as defined in Eq. (5).

$$P_g = P_L - P_{PV} + P_b \tag{5}$$

The power balance follows the following sign convention: $P_b > 0$ if the battery is charging, considering it as a load, and $P_g > 0$ if the power is absorbed from the grid.

The first step of the simulation of this reference case consists of the definition of initial SOC of each unit's battery; it is usually extracted from the database or set by the user depending on the simulation purpose.

The second step consists of the calculation of the difference between production and consumption (ΔP).

In step three, the battery power P_b and the corresponding SOC are calculated, according to the battery model.

In step four, the power balance (Eq. (5)) is applied at unit-level and the grid power flows are calculated.

Fig. 3 provides an example of baseline operation at unit-level. The simulation is 3-day long and uses forecasts data from July 11 to July 14 2024.

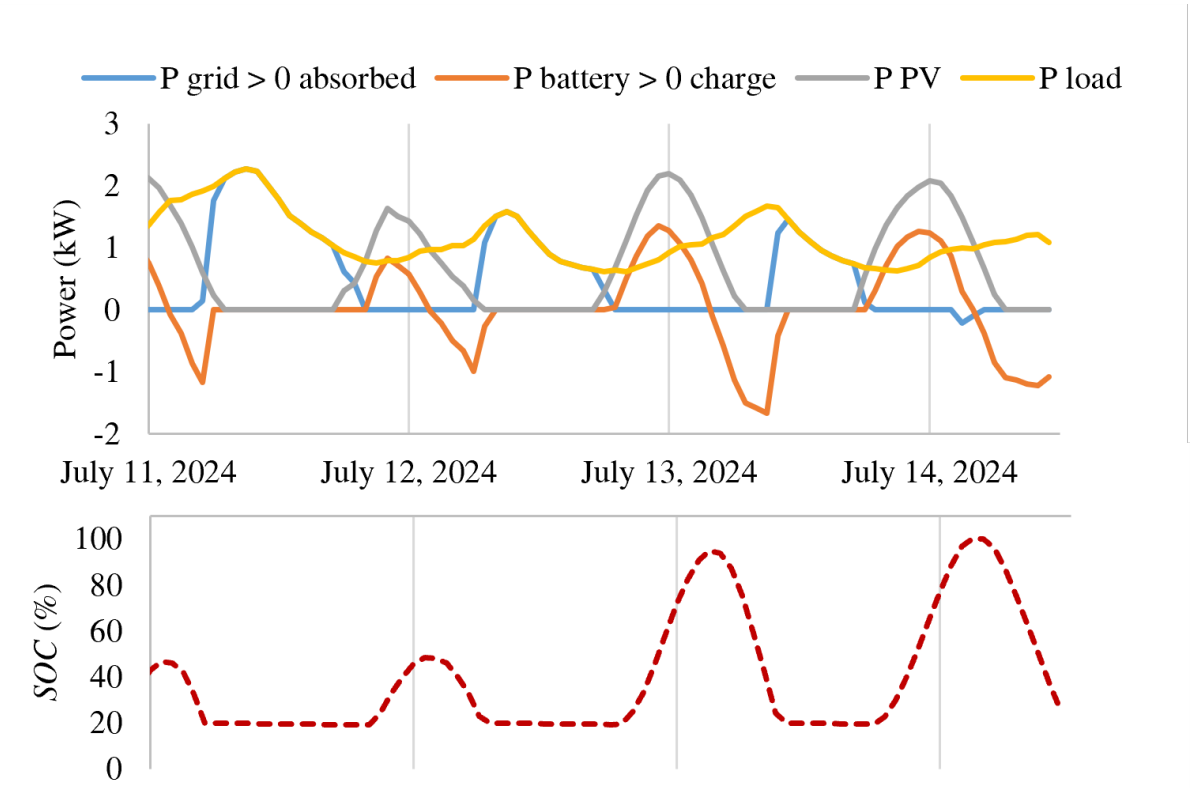

Figure 3: Baseline scenario - Unit 2

5.2 Optimized strategy for centralized management

The proposed optimization strategy aims to maximize self-sufficiency of the whole microgrid, by coordinating the energy exchanged between the units.

The self-sufficiency is defined as in Eq. (6), where $E_{grid,abs}$ is the total energy absorbed from the grid and E_{load} is the total energy consumed by the load.

$$\mathrm{SS}_{\mathrm{micro}} = 1 - \frac{E_{\mathrm{grid,abs}}}{E_{\mathrm{load}}} \tag{6}$$

The core of the strategy is the use of a non-linear programming solver (in MATLAB environment) that finds the minimum of a constrained objective function, given linear and non-linear constraints [16]. In this strategy, the objective function calculates the self-sufficiency of the entire system, while the non-linear constraints are related to the

behaviour of the battery (Eq. (3) and Eq. (4)). The output of the optimization function are the hourly battery power flows that fulfil the requirements and constraints. Then, through unit-level power balances (Eq. (5)), the grid power flows are calculated and the microgrid self-sufficiency computed.

In the first step, the initial battery power and *SOC* are defined. The battery power array is initialized as the array resulting from the baseline case, while the initial *SOC* condition is established as the same of the baseline case.

In the second step, the battery lower and upper boundaries (LB, UB) are defined. The LB corresponds to the battery maximum power of discharge, while the UB to the battery maximum power of charge.

In the third step, the battery non-linear conditions over the *SOC* are defined, by calculating the *SOC* limits through the function of Eq. (7), where x is the battery energy flows array under optimization, according to the battery model (Eq. (3), Eq. (4)).

$$\begin{aligned} \mathrm{SOC_lim}(x) = \ & \mathrm{F}(x, \eta_{\mathrm{char}}, \eta_{\mathrm{disch}}, C_{\mathrm{batt}}, P_{\mathrm{self_disch}}, \\ & \Delta t, \mathrm{SOC}_{\mathrm{max}}, \mathrm{SOC}_{\mathrm{min}}, \mathrm{SOC}_{\mathrm{in}}) \end{aligned} \tag{7}$$

In the fourth step, the self-sufficiency is maximized and batteries power flows calculated, according to Eq. (8).

$$P_{\mathrm{batt,opt}} = \max[\mathrm{SS}_{\mathrm{micro}}(PV_{\mathrm{t,n}}, Load_{\mathrm{t,n}}, \mathrm{BESS}_{0,n}, \mathrm{SOC}_{\mathrm{lim}})] \tag{8}$$

The final step consists of the calculation of the grid power through the balance of PV generation, consumption and battery power. Fig. 4 provides an example of application of the optimised strategy at unit-level.

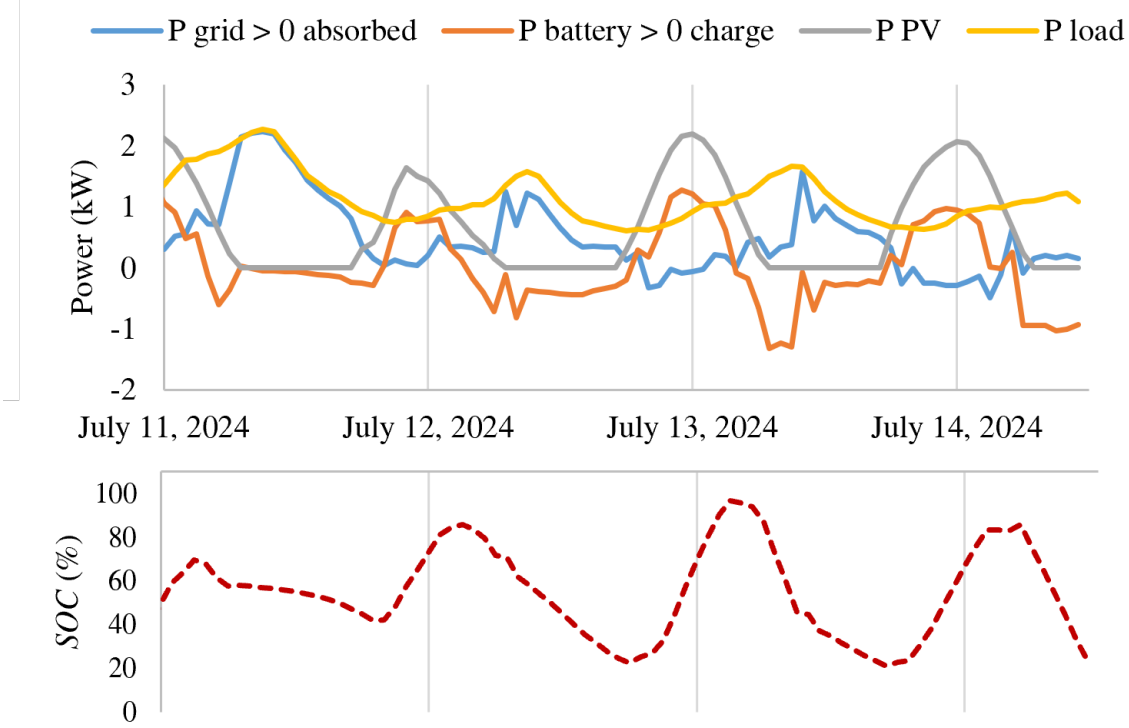

Figure 4: Optimised scenario - Unit 2

6 Simulation results

Thanks to the weather forecasts, the optimised strategy anticipates future energy availability peaks from the battery and balances its charging and discharging power accordingly. The main outcome of this control strategy is the balancing of the *SOC* levels among the community batteries, which tend to converge towards an intermediate value. When a prosumer is expected to experience a PV power peak in the near future, it discharges part of its battery storage to supply other users. These users are coordinated to absorb the energy, thus reducing the energy exchange with the external grid.

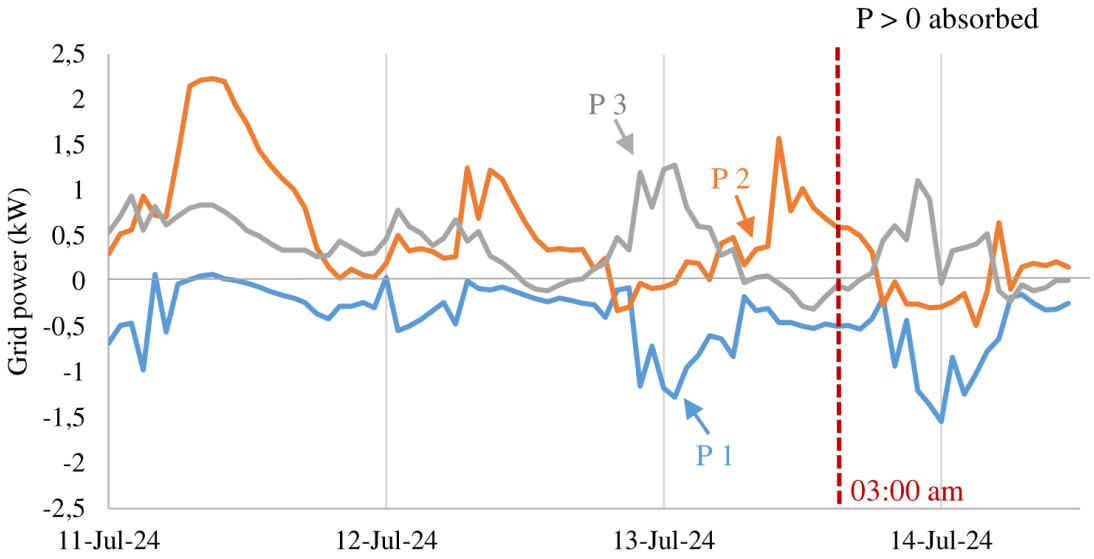

Figure 5: Highlight of grid power exchange correlations in deficit

Table 1: Grid Power in a deficit phase

Time	**Unit 1**	**Unit 2**	**Unit 3**
03:00	-447 W	457 W	31 W
04:00	-343 W	431 W	59 W
05:00	-408 W	270 W	145 W
06:00	-561 W	570 W	22 W

Table 2: Grid Power in a surplus phase

Time	**Unit 1**	**Unit 2**	**Unit 3**
09:00	-68 W	-286 W	340 W
10:00	-1155 W	-26 W	1198 W
11:00	-712 W	-81 W	817 W
12:00	-1174 W	-61 W	1225 W

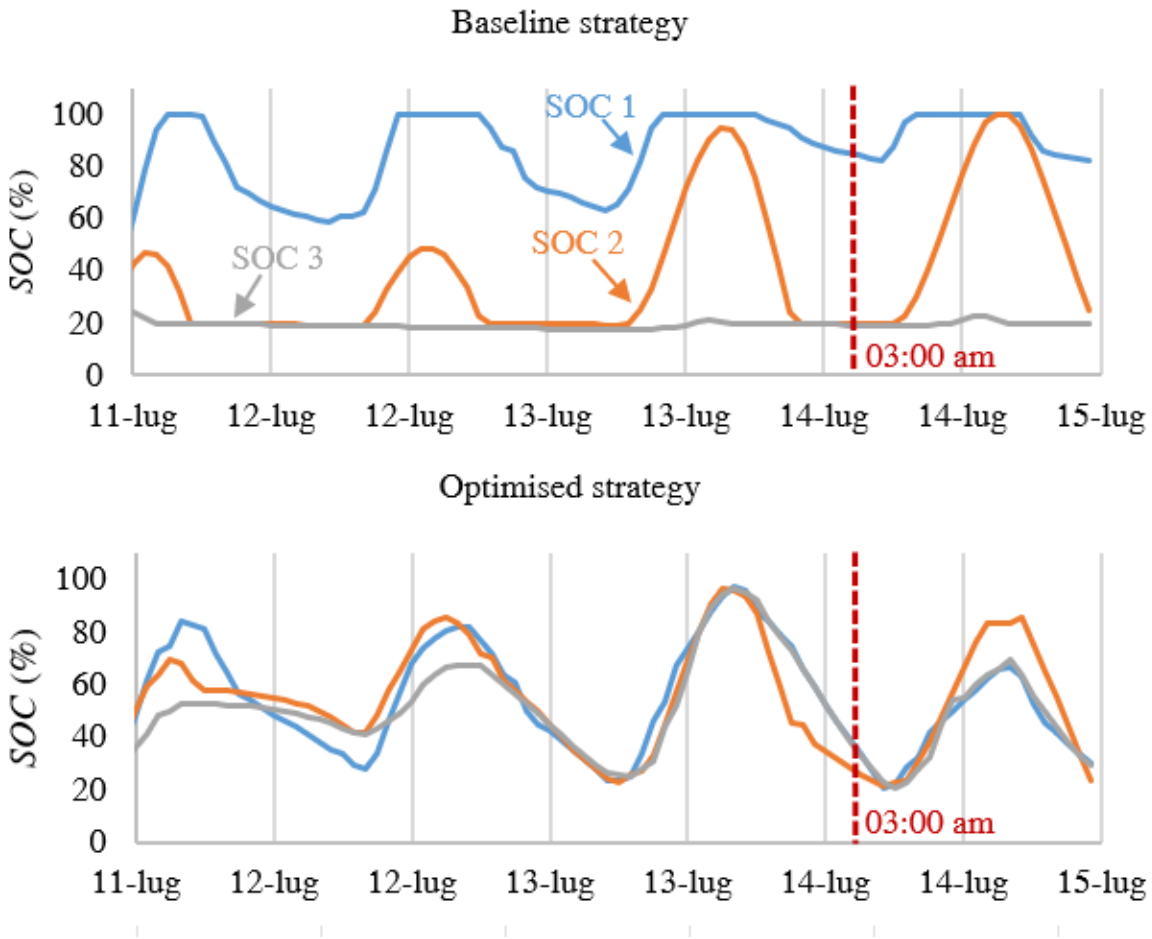

Figure 6: Comparison of *SOC* profiles in baseline and optimized strategy

6.1 Overall results

The results of the simulation over three days (July 11-14 2024) are provided in Table 3 and Table 4, for both single units and the whole microgrid. As was the aim of the strategy, the self-sufficiency for the whole system increased from 58% to 72% with the optimized one, while the self-consumption increased from 70% to 87%. Also a reduction of energy absorption from the external grid is registered from 73 kWh to 46 kWh.

Table 3: Results for the baseline strategy

Unit	**PV (kWh)**	**Load (kWh)**	**INJ (kWh)**	**ABS (kWh)**	***SC (%)***	***SS (%)***
Unit 1	60	20	31	0	33	100
Unit 2	60	99	1	43	94	57
Unit 3	15	44	0	30	100	34
Total	135	164	32	73	70	58

Table 4: Results for the optimized strategy

Unit	**PV (kWh)**	**Load (kWh)**	**INJ (kWh)**	**ABS (kWh)**	***SC (%)***	***SS (%)***
Unit 1	60	20	38	0	32	98
Unit 2	60	99	5	46	89	54
Unit 3	15	44	2	33	75	25
Total	135	164	11	46	87	72

7 Conclusions

This work presented a centralized energy management strategy for the PVZEN microgrid, aimed at maximizing microgrid self-sufficiency through a non-linear optimization algorithm. Simulations demonstrated a significant improvement in system performance: the self-sufficiency increased from 58% to 72%, while self-consumption rose from 70% to 87%. The coordinated control enabled the distributed batteries to operate as a virtual shared storage, ensuring more balanced *SOC* profiles, and improved storage availability during both surplus and deficit phases. This resulted in reduced reliance on the external grid and more effective utilization of local PV generation.

Future developments will integrate real-time transmission of optimized set-points to physical devices in the PVZEN lab, with a correction layer to compensate for forecasting errors and enhance energy balancing and system autonomy.

References

[1] X. Zhou, T. Guo, and Y. Ma, "An overview on microgrid technology," in *2015 IEEE International Conf. on Mechatronics and Automation (ICMA)*, Aug. 2015, pp. 76–81.

[2] L. Mariam, M. Basu, and M. F. Conlon, "Microgrid: Architecture, policy and future trends," *Renewable and Sustainable Energy Reviews*, vol. 64, pp. 477–489, Oct. 1, 2016.

[3] D. Menniti, N. Sorrentino, A. Pinnarelli, P. Vizza, G. Brusco, and G. Barone, "Sharing energy management model for renewable community self-consumption," in *2020 17th International Conf. on the European Energy Market (EEM)*, Sep. 2020, pp. 1–6.

[4] A. M. Saatloo, M. A. Mirzaei, and B. Mohammadi-Ivatloo, "A robust decentralized peer-to-peer energy trading in community of flexible microgrids," *IEEE Systems Journal*, vol. 17, no. 1, pp. 640–651, Mar. 2023.

[5] N. Hashemipour, P. C. D. Granado, and M. H. Sønju, "Comparing optimization strategies in local electricity markets," in *2022 18th International Conf. on the European Energy Market (EEM)*, Sep. 2022, pp. 1–7.

[6] H. Nagpal, I.-I. Avramidis, F. Capitanescu, and A. G. Madureira, "Local energy communities in service of sustainability and grid flexibility provision: Hierarchical management of shared energy storage," *IEEE Transactions on Sustainable Energy*, vol. 13, no. 3, pp. 1523–1535, Jul. 2022.

[7] R. Sudhoff, S. Schreck, S. Thiem, and S. Niessen, "Implications of forecast uncertainty on the optimal operation of renewable energy communities," in *27th International Conf. on Electricity Distribution (CIRED 2023)*, vol. 2023, Jun. 2023, pp. 1275–1279.

[8] J. Schlund, N. Pflugradt, D. Steber, U. Muntwyler, and R. German, "Benefits of virtual community energy storages compared to individual batteries based on behaviour based synthetic load profiles," in *2018 IEEE PES Innovative Smart Grid Technologies Conf. Europe (ISGT-Europe)*, Oct. 2018, pp. 1–6.

[9] PVZEN. "PhotoVoltaic Zero Energy Network," PVZEN. (), [Online]. Available: `https://pvzen.polito.it/` (visited on 04/30/2025).

[10] A. Amato, A. Carullo, A. Ciocia, *et al.*, "The PVZEN lab for energy communities: Monitoring system for identification of photovoltaic/battery/converter energy models," *IEEE Transactions on Instrumentation and Measurement*, vol. 74, pp. 1–12, 2025.

[11] PVGIS. "Photovoltaic geographical information system (PVGIS) - european commission." (Sep. 23, 2024), [Online]. Available: `https://joint-research-centre.ec.europa.eu/photovoltaic-geographical-information-system-pvgis_en` (visited on 05/09/2025).

[12] S. B. Schujman, J. R. Mann, G. Dufresne, *et al.*, "Evaluation of protocols for temperature coefficient determination," in *2015 IEEE 42nd Photovoltaic Specialist Conf. (PVSC)*, Jun. 2015, pp. 1–4.

[13] Martin Murnane and Adel Ghazel. "A closer look at state of charge (SOC) and state of health (SOH) estimation techniques for batteries | analog devices." (), [Online]. Available: `https://www.analog.com/en/resources/technical-articles/a-closer-look-at-state-of-charge-and-state-health-estimation-tech.html` (visited on 05/09/2025).

[14] A. Amato, A. Carullo, A. Ciocia, *et al.*, "The PVZEN laboratory for energy communities: Monitoring system for model identification," in *2024 IEEE International Instrumentation and Measurement Technology Conf. (I2MTC)*, May 2024, pp. 1–6.

[15] P. Di Leo, G. Malgaroli, A. Amato, S. Schubert, A. Ciocia, and F. Spertino, "An academic laboratory for all-electric energy communities: The case study of PVZEN microgrid," in *2023 IEEE 64th International Scientific Conf. on Power and Electrical Engineering of Riga Technical University (RTUCON)*, Oct. 2023, pp. 1–6.

[16] Mathworks. "fmincon - Find minimum of constrained nonlinear multivariable function - MATLAB." (), [Online]. Available: `https://it.mathworks.com/help/optim/ug/fmincon.html` (visited on 05/05/2025).